



Development of transgenic mice overexpressing mouse carbonyl reductase 1

Minako Yokoyama¹ · Toshitsugu Fujita² · Yuka Kadonosawa¹ · Yota Tatara³ · Daisuke Motooka⁴ · Masahito Ikawa⁴ · Hodaka Fujii² · Yoshihito Yokoayama¹

Received: 6 May 2022 / Accepted: 29 September 2022
© The Author(s), under exclusive licence to Springer Nature B.V. 2022

Abstract

Background Carbonyl reductase 1 (CBR1) is a nicotinamide adenine dinucleotide phosphate (NADPH)-dependent reductase with broad substrate specificity. CBR1 catalyzes the reduction of numerous carbonyl compounds, including quinones, prostaglandins, menadione, and multiple xenobiotics, while also participating in various cellular processes, such as carcinogenesis, apoptosis, signal transduction, and drug resistance. In this study, we aimed to generate transgenic mice overexpressing mouse Cbr1 (mCbr1), characterize the mCbr1 expression in different organs, and identify changes in protein expression patterns.

Methods and Results To facilitate a deeper understanding of the functions of CBR1, we generated transgenic mice overexpressing CBR1 throughout the body. These transgenic mice overexpress 3xFLAG-tagged mCbr1 (3xFLAG-mCbr1) under the CAG promoter. Two lines of transgenic mice were generated, one with 3xFLAG-mCbr1 expression in multiple tissues, and the other, with specific expression of 3xFLAG-mCbr1 in the heart. Pathway and network analysis using transgenic mouse hearts identified 73 proteins with levels of expression correlating with mCbr1 overexpression. The expression of voltage-gated anion channels, which may be directly related to calcium ion-related myocardial contraction, was also upregulated.

Conclusion mCbr1 transgenic mice may be useful for further in vivo analyses of the molecular mechanisms regulated by Cbr1; such analyses will provide a better understanding of its effects on carcinogenesis and cardiotoxicity of certain cancer drugs.

Keywords Cancer · CBR1 · Protein expression · Transgenic mice

Introduction

Carbonyl reductase 1 (CBR1) is a nicotinamide adenine

dinucleotide phosphate (NADPH)-dependent reductase with broad substrate specificity [1]. This enzyme catalyzes the reduction of various carbonyl compounds, including quinones, prostaglandins, menadione, and various xenobiotics. CBR1 regulates prostaglandin E2 (PGE2), which is important for proliferation and angiogenesis [2], catalyzes the reduction of the anticancer anthracyclines doxorubicin and daunorubicin, and enhances the production of the cardiotoxic substances doxorubicinol and daunorubicinol [2–5]. Inhibitors of CBR1 have been shown to cause the accumulation of reactive aldehydes and enhance oxidative stress, thus, altering tissue responses. Therefore, new substrates and inhibitors are being investigated to inhibit the negative effects of CBR1 [6–8].

We have previously shown that PGE2 is involved in cancer cell proliferation and angiogenesis [9], and that higher CBR1 expression is associated with a better prognosis in female cancer patients [10]. Furthermore, overexpression of

✉ Yoshihito Yokoayama
yokoyama@hirosaki-u.ac.jp

¹ Department of Obstetrics and Gynecology, Graduate School of Medicine, Hirosaki University, 5 Zaifu-cho, 036-8562 Hirosaki, Aomori, Japan

² Department of Biochemistry and Genome Biology, Graduate School of Medicine, Hirosaki University, 5 Zaifu-cho, 036-8562 Hirosaki, Aomori, Japan

³ Department of Stress Response Science, Center for Advanced Medical Research, Graduate School of Medicine, Hirosaki University, 5 Zaifu-cho, 036-8562 Hirosaki, Aomori, Japan

⁴ Genome Information Research Center, Research Institute for Microbial Diseases, Osaka University, 3-1 Yamadaoka, 565-0871 Suita, Osaka, Japan

human CBR1 (hCBR1) in human ovarian cancer cells was found to inhibit cell growth [11, 12], and hCBR1 inhibits the development of certain malignancies, such as cervical cancer, uterine sarcoma, and non-small cell lung carcinoma [13–15]. Thus, CRB1 protein might be used as a potential anticancer drug. In considering such treatment, it will be important to evaluate the effects of increased levels of CBR1 in the whole body to estimate its side effects.

The aim of this study was to generate transgenic mice overexpressing mouse *Cbr1* (mCbr1), characterize mCbr1 expression in various organs, and use a proteomic approach to identify changes in protein expression patterns in these transgenic mice. In future, these mice might be useful for examining the inhibitory effect of mCbr1 overexpression on carcinogenesis (e.g., ovarian cancer) by mating with mouse models of cancer.

Materials and methods

Generation of transgenic mouse lines

The coding region of *mCbr1* in pCMV6-AC-GFP-mCbr1 (OriGene, Rockville, MD, USA) was amplified by PCR using primer No. 7 and 8 (Table S1). The amplicon was inserted between the *NotI* and *EcoRV* sites in p3xFLAG-CMV7.1 (Sigma-Aldrich, Tokyo, Japan) using In-Fusion HD Cloning Kits (Takara Bio, Inc., Kusatsu, Japan). The resulting plasmid p3xFLAG-CMV7.1-mCbr1 was digested with *Eco53KI* and *SaII* to construct pCAG1.1-3xFLAG-mCbr1, and the coding region of *3xFLAG-mCbr1* was cloned into the *EcoRV* and *SaII* sites of pCAG1.1 [16]. pCAG1.1-3xFLAG-mCbr1 was digested with *SacI* and *PacI*, and the expression cassette, including the CAG promoter and *3xFLAG-mCbr1* (Figure S1), was microinjected into the pronuclei of C57BL/6 N fertilized eggs. The injected eggs were transferred to the oviducts of pseudopregnant ICR female mice. Three weeks after birth, a tailpiece of each mouse was subjected to genomic DNA (gDNA) extraction followed by genotyping PCR to confirm germline transmission. All animal experiments were approved by the Institutional Animal Care and Use Committee at the Research Institute for Microbial Diseases, Osaka University (4111) and Hirosaki University (M19024). This study complied with the ARRIVE guidelines. All methods were performed in accordance with the relevant guidelines and regulations.

Genotyping

To genotype founder mice, gDNA was extracted from each mouse using DNeasy Blood & Tissue Kits (QIAGEN, Tokyo, Japan) and was subjected to PCR with KOD FX

(Toyobo Life Science, Osaka, Japan) and primer No. 11 and 12 (Table S1). The amplification protocol consisted of an initial denaturation at 94 °C for 2 min, followed by 30 cycles of denaturation at 98 °C for 10 s, annealing at 66 °C for 30 s, and extension at 68 °C for 1 min. After the first generation, mice were PCR genotyped using primer No. 16 and 12 (Table S1), with primer No. 27 and 33 used to confirm the insertion sites and No. 29 and 44 used to confirm the directions of the transgenes (Table S1). If necessary, amplicons were subjected to DNA sequencing analysis (Eurofins Genomics, Tokyo, Japan).

Quantification of the copy numbers of the transgene

The number of copies of the *mCbr1* gene of each founder mouse, was evaluated by real-time PCR with gDNA using Thunderbird SYBR qPCR Mix (Toyobo Life Science). Endogenous and transgenic *mCbr1* genes were amplified using primer No. 51 and 52 (Table S1). The number of copies of the *mCbr1* gene was normalized relative to that of the *GAPDH* gene, which was amplified using primer No. 26576 and 26577 (Table S1). The relative copy number in transgenic mice was determined by comparison with the number of copies of the endogenous *mCbr1* gene in wild type (WT) mice. In this context, the numbers of the transgene can be calculated by subtraction of that of the endogenous gene (two copies).

Next-generation sequencing (NGS) analysis

Whole-genome sequencing was performed to examine the insertion sites of the transgenes in the genome. Libraries were prepared using the Illumina DNA PCR-Free Prep, Tagmentation (Illumina, San Diego, CA, USA). Sequencing was performed on the NovaSeq 6000 (Illumina). The NGS data were analyzed using Transgene R (<https://github.com/menggf/transgeneR>) [17] by Tohoku Chemical Co., Ltd. (Iwate, Japan). Then, the NGS data were mapped onto the reference genome GRCh38.

Analysis of insertion locations based on the information in NGS

DNA was PCR amplified using primers constructed at sites 40–300 bp from the insertion sites (No. 27 and 33, and No. 29 and 44; Table S1), followed by sequencing analysis of the resulting PCR products.

RNA extraction and reverse transcription (RT)

Total RNA was isolated from mouse organs using Isogen II (Nippon Gene, Tokyo, Japan), according to the manufacturer's protocol. RT reactions were performed with ReverTra Ace qPCR RT Master Mix with gDNA Remover (Toyobo Life Science). The resulting cDNA was subjected to quantitative real-time PCR using Thunderbird SYBR qPCR Mix (Toyobo Life Science). Endogenous and transgenic *mCbr1* cDNA were amplified using primer No. 51 and 52 (Table S1). The levels of *mCbr1* cDNA were normalized relative to those of 18S rRNA cDNA, which was amplified using primer No. 26773 and 26774 (Table S1). Differences between the three groups were determined by one-way ANOVA followed by Tukey's test, with $p < 0.05$ defined as statistically significant. All statistical analyses were performed using IBM SPSS ver. 26.0 statistics software (IBM, Chicago, Illinois).

Protein extraction and the immunoblot analysis

The mice were euthanized, and eight organs (brain, heart, lung, liver, spleen, kidney, uterus, and ovary) were removed. Each organ was homogenized on ice in RIPA buffer (Fujifilm Wako, Osaka, Japan) containing protease inhibitors (cOmplete Tablets, Mini EDTA-free EASY pack, Roche, Basel, Switzerland). Equal amounts of protein were loaded on 5–20% SDS-polyacrylamide gels (Fujifilm Wako), electrophoresed, and transferred to polyvinylidene difluoride membranes. After blocking with Tris buffer saline (TBS) containing 0.05% Tween-20 and 5% skim milk, the membranes were incubated overnight at 4 °C with primary antibody, either anti-CBR1 (ab-186825, Abcam, Cambridge, UK), anti-GAPDH (014-25524, Fujifilm Wako) or anti- β -actin (M177-3, MBL, Tokyo, Japan). After washing with TBS containing 0.05% Tween-20, the membranes were incubated with the appropriate horseradish peroxidase (HRP)-conjugated secondary antibody, either anti-rabbit IgG-HRP (NA9340V, GE Healthcare, Pittsburgh, PA) or anti-mouse IgG-HRP (NA9310V, GE Healthcare). ECL Prime (GE Healthcare) was used for detection of proteins of interest with chemiluminescent signals.

Immunohistochemistry

For immunohistochemical examination, hearts were fixed with formalin, embedded in paraffin. They were then sectioned at a thickness of 4 μ m; the sections were mounted on saline-coated glass slides. Deparaffinized sections were incubated with a rabbit polyclonal anti-CBR antibody (NBP1-86595, Novus Biologicals, Colorado) using the BOND polymer refine detection system (Leica

BOND-MAX). The tissue sections were subsequently stained with 3,3'-diaminobenzidine (DAB) and counterstained with hematoxylin.

Cellular proteomic analysis of hearts by liquid chromatography (LC)-mass spectrometry (MS)/MS

Proteins were extracted from the hearts of WT and transgenic mice ($n = 3$ each), as described above. The concentrations of extracted proteins were determined using the BCA method, with albumin as the standard protein. Sample volumes were adjusted so that each sample contained 20 μ g of protein, and the proteins were precipitated with chilled acetone. These proteins were denatured with 50% trifluoroethanol, followed by reduction and alkylation. The proteins were incubated with trypsin, and the resulting peptides were desalted and subjected to LC-MS/MS using a nanoLC Eksigent 400 system (AB Sciex, Framingham, MA, USA), coupled online to an TripleTOF6600 mass spectrometer (AB Sciex).

Data analysis

Acquired spectra were searched against the UniProt database using the Paragon algorithm embedded in ProteinPilot 5.0.1 software program (AB Sciex). The search parameters consisted of (i) sample type: identification, (ii) Cys alkylation: iodoacetamide, (iii) digestion: trypsin, (iv) instrument: TripleTOF 6600, (v) species: *Mus musculus*, (vi) ID focus: biological modifications, and (vii) detected protein threshold: >0.05 (10% confidence). To enable curve fitting using an independent FDR analysis [18], the detected protein threshold was set at the minimum level to enhance the number of wrong answers. Positive identifications were considered when identified proteins and peptides reached a 1% local FDR [19]. The resulting group file was loaded into PeakView (ver. 2.2.0, AB Sciex), and peaks from SWATH runs were extracted with a peptide confidence threshold of 99% and a false discovery rate of $<1\%$. The SWATH files were exported to MarkerView software program (ver. 1.3.0.1; AB Sciex), and the peak areas of individual peptides were normalized relative to the sum of the peak areas of all detected peptides.

Statistical analysis

Proteomics data were analyzed by Welch's t-test in MarkerView 1.3 software (AB Sciex) to determine statistically significant differences in protein levels between experimental groups. Statistical significance was set at $p < 0.05$. Principal component analysis and orthogonal partial least square-discriminant analysis (OPLS-DA) were performed

as multivariate analyses using Simca software (Infocom Corp., Tokyo, Japan). Pareto scaling was applied to the normalized peak area values acquired by SWATH before the analyses, representing a compromise between the extremes of no scaling and unit variance scaling. After centering, each spectral variable was divided by the square root of its standard deviation. A principal component analysis score scatter plot of the first two principal component scores, which accounted for 55.0% of the original variation, is shown in Figure S2. There were no major outliers. In the proteomics dataset, good discriminant models were constructed using OPLS-DA (Figure S3); however, due to variations in *mCbr1* protein levels, proteins that correlated with levels of *mCbr1* were analyzed. Hierarchical clustering and correlation analyses were performed using R with the MetaboAnalyst package [20, 21]. Spearman's rank correlation was used to measure distance. The threshold for correlation and proteins seemingly related to *mCbr1* was set at a $-\log_{10}$ (p-value) that exceeded 1.3.

Network analysis using ingenuity pathway analysis (IPA)

Networks were generated by IPA (QIAGEN) using inputs of UniProt IDs and fold changes of significantly differentially regulated proteins ($p < 0.05$) or proteins that correlated with *CBR1* expression.

Results

Generation of transgenic mice overexpressing *mCbr1*

To generate transgenic mice expressing 3xFLAG-tagged [22, 23] *mCbr1* (3xFLAG-*mCbr1*), we constructed pCAG1.1-3xFLAG-*mCbr1*, a plasmid expressing 3xFLAG-*mCbr1* under the control of the CAG promoter. The 3xFLAG-*mCbr1* expression cassette of pCAG1.1-3xFLAG-*mCbr1* was microinjected into the pronuclei of fertilized eggs from C57BL/6 N mice to generate founders. Genotyping showed the presence of the transgene in five of the 37 founder mice (Figure S4). Crossing each of these founders with WT C57BL/6 N mice showed that two of the five did not produce next-generation mice possessing the transgene, and that one produced the third generation of crossed mice. However, half of the generated mice died within a few days of birth and the other half could not develop normally. We, therefore, discontinued our efforts of maintaining this strain. Nonetheless, two strains, No. 7 (Tg7) and No. 15 (Tg15) grew healthily and normally and survived for more than 2 years. The average litter sizes were 7.1 and 8.3 for Tg7 and

Tg15, 40.1% and 41.3% of which maintained the transgene, respectively. The sex ratios (male: female) of these offspring were 1: 0.79 and 1: 2.32 for Tg7 and Tg15, respectively. No apparent behavioral abnormalities were observed in either strain, and both were therefore established as lines.

Analysis of the copy number and insertion sites of the 3xFLAG-*mCbr1* transgenes.

Quantitative real-time PCR using equal amounts of gDNA from WT, Tg7, and Tg15 mice was performed to determine the number of 3xFLAG-*mCbr1* transgene copies in each of these mice. Based on the number of *mCbr1* copies in WT mice, the mean relative numbers of copies in Tg7 and Tg15 mice were 2.73 and 4.78, respectively (Fig. 1a), indicating that one and three copies of the 3xFLAG-*mCbr1* transgene had been inserted into the genomes of Tg7 and Tg15 mice, respectively. Next, NGS analysis using gDNA from Tg7 and Tg15 mice was performed to determine the insertion sites of the transgene. Three potential insertion sites on chromosome 4 (3,089,737; 3,090,085; and 3,090,920) were identified in Tg7 mice, and two insertion sites on chromosome X (75,970,745 and 75,973,675) were identified in Tg15 (Fig. 1b). In Tg7 mice, one copy of the 3xFLAG-*mCbr1* transgene was inserted into one of these potential insertion sites on chromosome 4 (Fig. 1a and b). Since these potential insertion sites are present within a repeat sequence region, we were unable to design an appropriate primer set to confirm the insertion site. In Tg15, three copies of the 3xFLAG-*mCbr1* transgene may have been inserted into one of the two potential insertion sites on chromosome X (Fig. 1a and b). Alternatively, two copies may have been inserted into one potential insertion site and one copy into the other site. Insertion sites and directions of insertion were assessed by genotyping PCR. Genotyping PCR with two primer sets was found to successfully amplify the target DNA regions (Figure S5). The amplified DNA sequences were further confirmed by DNA sequencing. These results show that two transgene copies have been inserted into each site as identified by NGS analysis, although the insertion pattern of the third copy remains unclear. Notably, no coding genes were detected between the identified insertion sites.

Confirmation of overexpression of the 3xFLAG-*mCbr1* mRNA and protein

The levels of 3xFLAG-*mCbr1* mRNA expression were evaluated in eight organs (brain, heart, lung, liver, spleen, kidney, uterus, and ovary) of female mice by RT followed by quantitative real-time PCR (Fig. 2). Abundant expression of *mCbr1* mRNA was observed in the hearts of Tg7 mice, and in the brains, hearts, lungs, kidneys, and ovaries

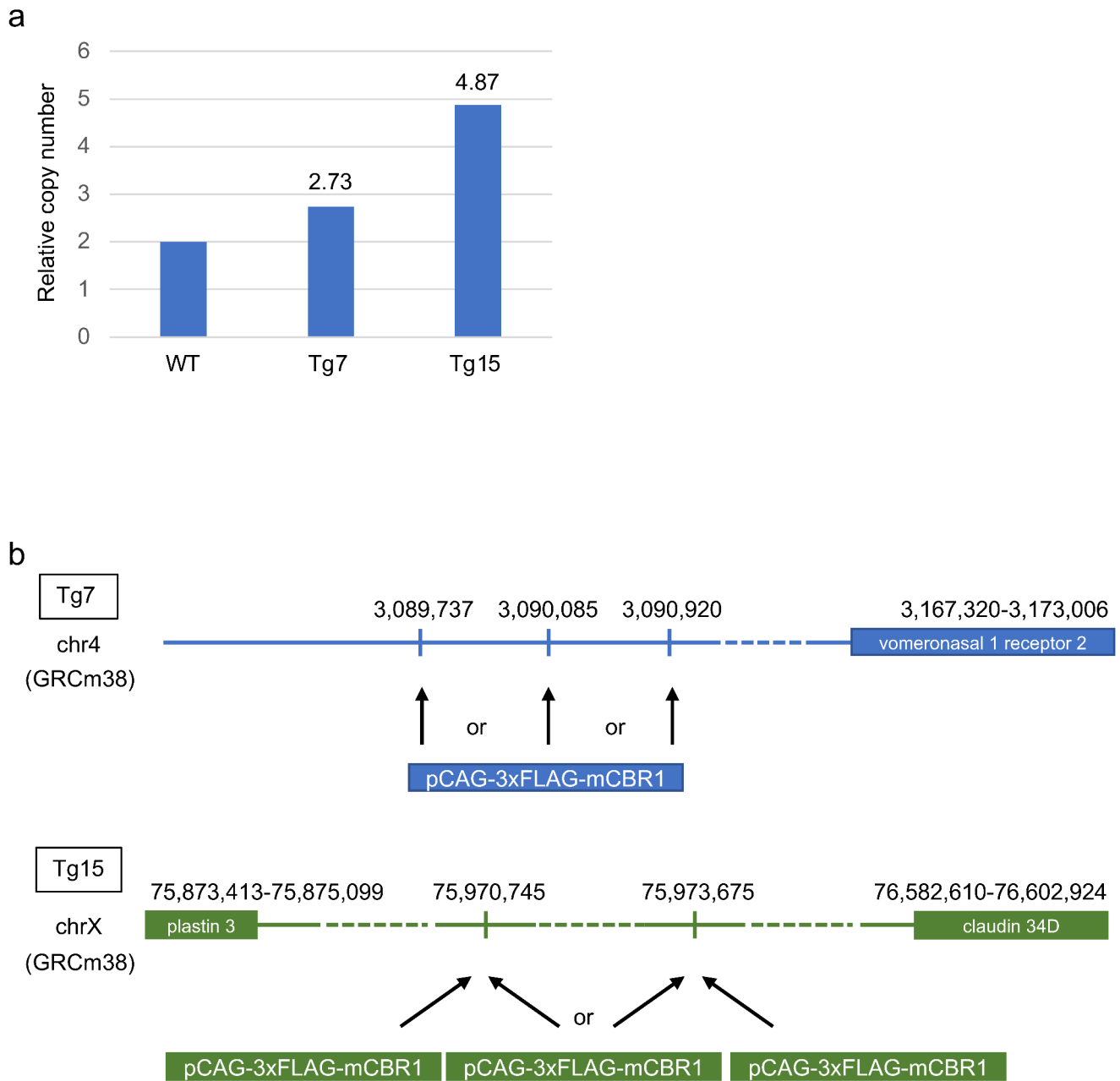


Fig. 1 Copy numbers and insertion sites of the *3xFLAG-mCbr1* gene in transgenic mouse lines

(a) Number of *mCbr1* gene copies. gDNA samples of WT, Tg7, and Tg15 mice were subjected to real-time quantitative PCR to determine the number of copies of the *mCbr1* gene. The relative number of copies of *3xFLAG-mCbr1* in Tg7 and Tg15 mice was calculated based on

of Tg15 mice. Next, the immunoblot analysis using an anti-Cbr1 antibody was performed to compare expression levels of mCbr1 proteins. The immunoblot analysis showed that the 3xFLAG-mCbr1 protein was overexpressed only in the hearts of Tg7 mice, but more widely (brain, heart, lung, spleen, kidney, uterus, and ovary) in Tg15 mice (Fig. 3). Thus, both RT-PCR and the immunoblot analysis showed

the number of copies of *mCbr1* in WT mice (2 copies). (b) Schematic diagram showing the insertion sites of the *3xFLAG-mCbr1* transgene in transgenic mouse lines. Insertion sites were identified by NGS analysis. Based on the number of copies of *mCbr1* in WT mice, one copy of *3xFLAG-mCbr1* is inserted at the indicated site in Tg7 mice, and three copies are inserted at the indicated site in Tg15 mice

that 3xFLAG-mCbr1 was abundantly expressed in the hearts of both mouse lines.

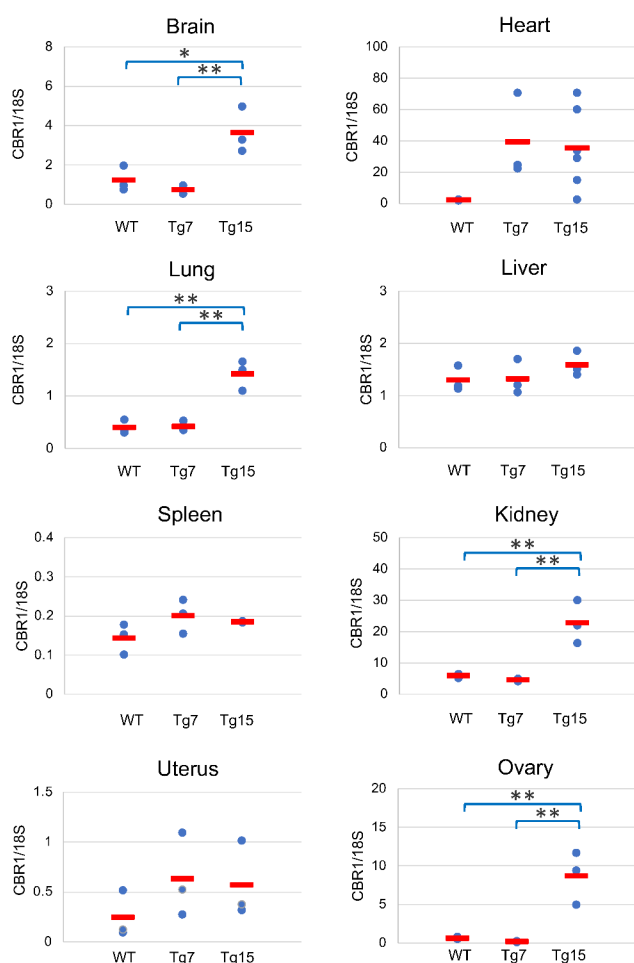


Fig. 2 *mCbr1* mRNA levels in the organs of transgenic mice
The mRNA expression levels of *mCbr1* in the eight indicated organs were determined by quantitative real-time PCR and were normalized relative to the levels of expression of *18S rRNA*. The mean levels ($n = 3$ or 6) of *mCbr1* mRNA were calculated and are shown as red horizontal lines. * $p < 0.05$, ** $p < 0.01$ vs. WT, calculated using one-way ANOVA followed by Tukey's test

Evaluation of mCbr1 protein expression in the myocardium by immunostaining

Considering that mCbr1 was abundantly expressed in the hearts of transgenic mice, we evaluated the expression of mCbr1 in the myocardium of female mice by immunostaining (Fig. 4). In transgenic mice, mCbr1 expression increased in the heart muscle bundles of the ventricles. Interestingly, the hearts of Tg15 mice showed a mixture of strongly stained and unstained cells, which could be attributed to the *3xFLAG-mCbr1* transgenes inserting into chromosome X, with one X chromosome in each cell being inactivated randomly during cellular differentiation (X chromosome inactivation). Images of tissue sections showed a tendency toward hypertrophy in the hearts of Tg7 and Tg15 mice,

although differences between these mice and WT mice were marginal.

Alteration of protein expression patterns by overexpression of 3xFLAG-mCbr1

Lastly, we examined how overexpression of 3xFLAG-mCbr1 affects cellular homeostasis. Quantification of protein expression in the hearts of WT and transgenic mice by mass spectrometry analysis revealed that overexpression of 3xFLAG-mCbr1 altered the expression levels of 1,169 proteins. Spearman's rank correlation coefficient analyses showed that overexpression of 3xFLAG-mCbr1 correlated with the expression level of 73 proteins ($p < 0.05$) and strongly correlated with the expression level of 20 proteins ($p < 0.01$; Fig. 5a). mCbr1 expression correlated positively with the expression of the calcium channel-related protein ryanodine receptor 2 (RYR2), mitochondrial-related protein mitochondrial 2-oxoglutarate/malate carrier protein (SLC25A11), NADH dehydrogenase [ubiquinone] 1 alpha subcomplex subunit 1 (NDUFA1), and NDUFA13. Pathway analysis of these 73 proteins using IPA revealed that the expression of mitochondria-related proteins, specifically voltage-gated anion channels, such as VDAC1 and VDAC2, was upregulated. Network analysis confirmed the enhanced expression of VDAC1 and VDAC2, as well as a calcium channel-related protein (RYR2), which have important roles in triggering myocardial contraction (Fig. 5b). Thus, overexpression of 3xFLAG-mCbr1 altered several protein expression patterns in the heart, which may affect cellular signaling networks.

Discussion

In this study, we generated two lines of transgenic mice expressing mCbr1 and evaluated the changes in protein expression patterns in the hearts of these mice. Our results showed that the expression of proteins related to calcium channels, RYR2-related proteins, VDAC1, and VDAC2 was altered.

We had previously reported that hCbr1-overexpressing cancer cell xenografts showed delayed growth in mice, whereas cancer cells in which CBR1 expression was knocked down showed active growth and invasion [11, 12, 24]. In addition, analysis of peritoneal metastasis of ovarian cancers using artificial peritoneal tissues showed that the growth of hCbr1-overexpressing ovarian cancer cells was inhibited, and cell death was enhanced [25]. These findings suggest that the mCbr1 transgenic mice, especially Tg15, are useful for verifying the inhibitory effects of mCbr1 on cell growth and their molecular mechanisms in ovarian

a Blot: anti-CBR1

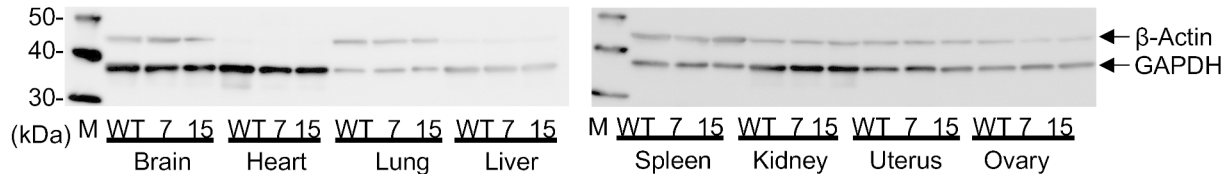
b Blot: anti- β -Actin and anti-GAPDH

Fig. 3 Abundance of mCbr1 proteins in transgenic mouse lines (a) Levels of mCbr1 protein abundance in the eight indicated organs, as determined by immunoblot analysis. (b) Expression levels of

β -actin and GAPDH proteins in these samples, as determined by the immunoblot analysis
*: Nonspecific bands

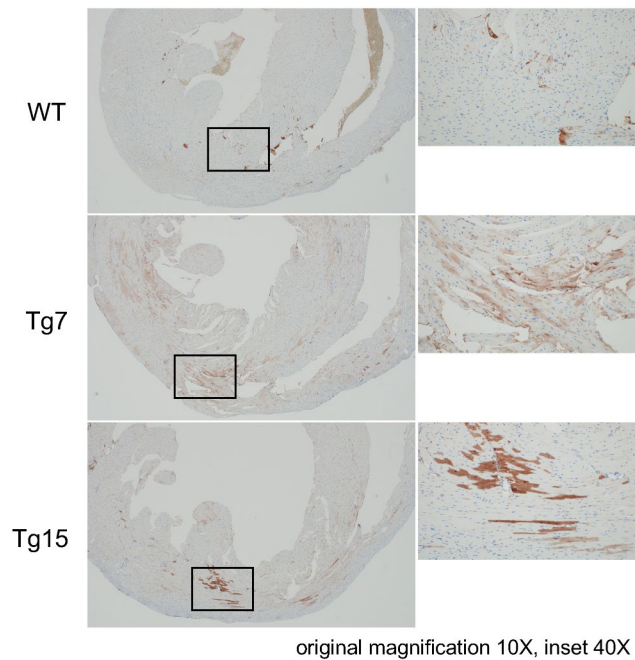


Fig. 4 Abundance of mCbr1 protein in transgenic mouse hearts
Immunohistochemical assessment of mCbr1 protein abundance in mouse hearts (original magnification, 10 \times , inset 40 \times). Female mice aged 16–18 weeks were used; Tg7, the third generation and Tg15, the second generation

cancer cells. These molecular mechanisms may be further revealed by mating Tg15 mice overexpressing mCbr1 in the ovaries with transgenic mice that develop ovarian cancers in an age-dependent manner [26].

In the present study, to generate mCbr1 transgenic mice, we expressed 3xFLAG-mCbr1 under the control of the CAG promoter. 3xFLAG-mCbr1 was detected in multiple tissues, predominantly within the hearts of Tg15 mice and solely

in the hearts of Tg7 mice. This pattern of expression may be due to the characteristics of the CAG promoter, which may be more activated in muscle tissues [16]. The mCbr1 transgenes were inserted into chromosome X in Tg15 mice. Since one X chromosome is randomly inactivated in each cell of female mice, the mCbr1 transgenes were not expressed in half of their cells. However, this inactivation was not observed in male Tg15 mice.

CBR1-mediated metabolites of anthracycline anticancer drugs have been found to induce cardiotoxicity. For example, CBR1 reduces daunorubicin from its 13-ketone form to its 13-hydroxy metabolite (daunorubicinol), which is both less effective and cardiotoxic [6, 27, 28–30]. Evaluation of the molecular mechanisms underlying CBR1-mediated signaling pathways in the heart is necessary to improve the therapeutic efficacy of anthracycline anticancer drugs and to minimize their cardiotoxicity. Since we found that mCbr1 is highly expressed in the hearts of mCbr1 transgenic mice, these mice will be useful in characterizing these molecular mechanisms. Transgenic mice expressing hCBR1 in their hearts have also been developed [5]. Although the amino acid sequences of hCBR1 and mCbr1 are 87% identical, it may be ideal to generate transgenic mice overexpressing allogeneic Cbr1 in the heart. Considering that the cardiotoxicity of anthracycline anticancer drugs and their inhibitors have been extensively studied [31–37], these transgenic mice will facilitate the identification of potential strategies to reduce anthracycline anticancer drug-induced adverse events and cardiotoxicity.

The results of the network analysis showed that the levels of calcium channel-related protein expression, such as RYR2, and mitochondrial membrane proteins, such as VDAC1 and VDAC2, increased in proportion to the increase

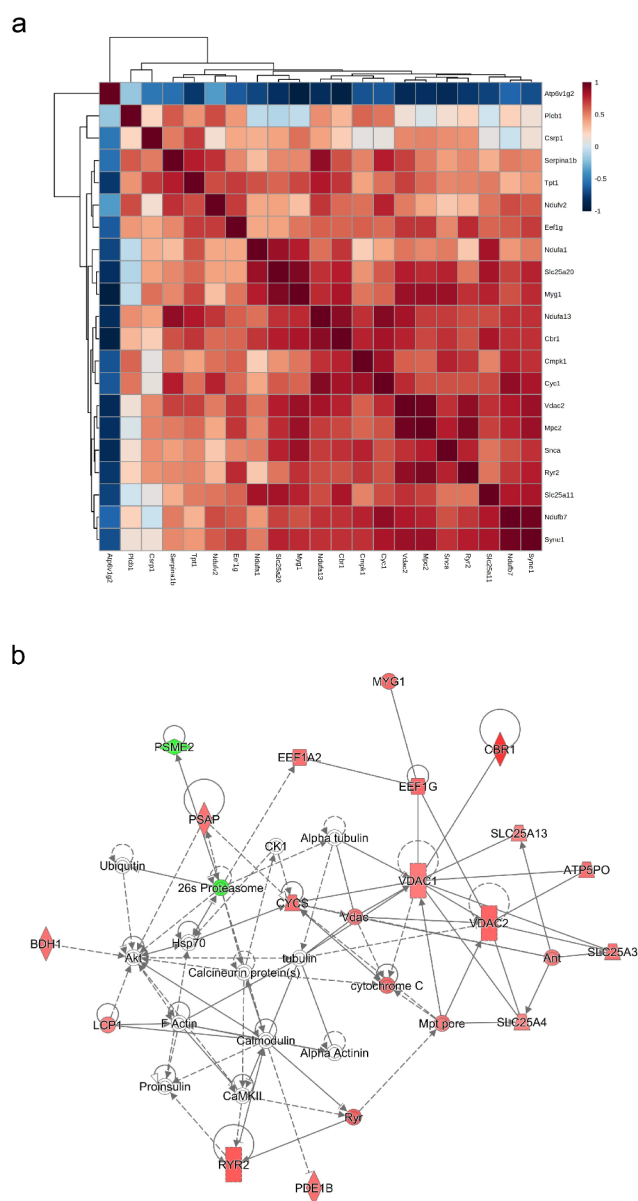


Fig. 5 Effects of mCbr1 overexpression on protein abundance in mouse hearts

Proteins were extracted from three hearts each from WT, Tg7, and Tg15 mice, and correlations between their levels of abundance and those of mCbr1 were analyzed by Spearman correlation coefficient. (a) Heatmap of myocardial proteins whose levels showed correlations with those of mCbr1. Of the 1,169 proteins detected in the myocardium using LC-MS/MS, 20 were correlated with mCbr1 ($p < 0.01$). Proteins with strong positive correlations are shown in red, and those with strong negative correlations are shown in blue. (b) Pathway and network analyses using IPA. Of the 1,169 proteins detected in the myocardium using LC-MS/MS, 73 were correlated with mCbr1 ($p < 0.05$). Potential signaling connections of these proteins are shown. Proteins positively and negatively correlating with CBR1 are shown in red and green, respectively

in mCbr1 in the heart. RYR2, a calcium channel in the sarcoplasmic reticulum membrane, is responsible for calcium

release from the sarcoplasmic reticulum and is expressed at high levels in cardiac muscle, smooth muscle, lung, and brain. Administration of doxorubicin has been shown to alter the expression of this ryanodine receptor [38]. VDAC is an anion channel on the outer membrane of mitochondria; it is responsible for the exchange of ions and small hydrophilic molecules between the inner and outer membranes [39]. VDAC is also involved in regulating interactions with other proteins and molecules in the mitochondria, thereby regulating intracellular metabolism [39]. The transgenic mouse model developed in the present study will facilitate future research elucidating the mechanism by which the expression of these proteins was upregulated thereby leading to a better understanding of the mechanism of action of CBR1 in vivo.

In this study, considering future examination of the inhibitory effect of mCbr1 overexpression on female-specific carcinogenesis by mating mouse models of cancer, we mainly analyzed the effects of mCbr1 overexpression in female transgenic mice. In the future, it would be interesting to analyze the effects of mCbr1 overexpression in male transgenic mice because a sex difference in the activity of CBR1 has been reported [40]. In addition, it is reported that CBR1 is related to Down syndrome (trisomy of chromosome 21) [41]. Because the *CBR1* gene is located on chromosome 21 in humans, three copies of the gene are present in individuals with Down syndrome. Studies using Down syndrome model mice showed that reversion of the copy number of the *Cbr1* gene to two copies alleviates the decrease in PGE2 and memory impairment [41], suggesting that CBR1 is one of the proteins responsible for Down syndrome. Because mCbr1 is overexpressed in the brain, the transgenic mice generated herein may also be useful for evaluating the relationship between CBR1 and Down syndrome.

In this study, we generated transgenic mice overexpressing mCbr1 in the heart and other organs. These transgenic mice will be useful for studying CBR1-mediated cancer suppression mechanisms, cardiotoxicity induced by metabolites of anticancer drugs in the heart, and Down syndrome.

Supplementary Information The online version contains supplementary material available at <https://doi.org/10.1007/s11033-022-07994-x>.

Acknowledgements The authors thank Hiroshi Kijima for his assistance with the immunohistochemistry analysis; Takeshi Shimizu, Shoko Nagata, and Hirotaaka Fujita for their technical assistance; and Miyu Miyazaki for her technical support in the mass spectrometry analysis.

Author contributions: M.Y., H.F., and Y.Y. conceived the project; T.F. and H.F. designed and supervised the project; Y.T. performed the LC-MS/MS analysis; D.M. performed the NGS analysis; M.I. generated the transgenic mice; M.Y. and Y.K. performed the other experiments; and M.Y., T.F., H.F., and Y.Y. wrote the manuscript. All authors have

read and approved the final version of the manuscript.

Data Availability NGS analysis data are available online using the accession number “DRA012939” for DDBJ/EMBL/GenBank. The proteomic data are available online using the accession number “PXD027170” for ProteomeXchange [42], and the accession number “JPST001246” for the jPOST repository [43].

Statements and Declarations

Funding None.

Competing Interests: Y.Y. and M.Y. have filed a patent application for the transgenic mice with details as follows: Name: Transgenic non-human animals; Number: Japanese Patent Application No. 2022-009381; Status: Under review; Specific aspect of manuscript covered in the patent application: All the information reported in this study.

Ethics approval: All animal experiments were approved by the Institutional Animal Care and Use Committee at the Research Institute for Microbial Diseases, Osaka University (4111) and Hirosaki University (M19024). This study complied with the ARRIVE guidelines. All methods were performed in accordance with the relevant guidelines and regulations.

Consent to participate: Not applicable.

Consent to publish: Not applicable.

References

- Persson B, Kallberg Y (2013) Classification and nomenclature of the superfamily of short-chain dehydrogenases/reductases (SDRs). *Chem Biol Interact* 202:111–115. <https://doi.org/10.1016/j.cbi.2012.11.009>
- Wermuth B (1981) Purification and properties of an NADPH-dependent carbonyl reductase from human brain. Relationship to prostaglandin 9-ketoreductase and xenobiotic ketone reductase. *J Biol Chem* 256:1206–1213. [https://doi.org/10.1016/S0021-9258\(19\)69950-3](https://doi.org/10.1016/S0021-9258(19)69950-3)
- Gonzalez-Covarrubias V, Kalabus JL, Blanco JG (2008) Inhibition of Polymorphic Human carbonyl reductase 1 (CBR1) by the cardioprotectant Flavonoid 7-monohydroxyethyl rutoside (monoHER). *Pharm Res* 25:1730–1734. <https://doi.org/10.1007/s11095-008-9592-5>
- Olson LE, Bedja D, Alvey SJ, Cardounel AJ, Gabrielson KL, Reeves RH (2003) Protection from doxorubicin-induced cardiac toxicity in mice with a null allele of carbonyl reductase 1. *Cancer Res* 63:6602–6606
- Forrest GL, Gonzalez B, Tseng W, Li X, Mann J (2000) Human carbonyl reductase overexpression in the heart advances the development of doxorubicin-induced cardiotoxicity in transgenic mice. *Cancer Res* 60:5158–5164
- Shi SM, Di L (2017) The role of carbonyl reductase 1 in drug discovery and development. *Expert Opin Drug Metab Toxicol* 13:859–870. <https://doi.org/10.1080/17425255.2017.1356820>
- Hu D, Miyagi N, Arai Y, Oguri H, Miura T, Nishinaka T et al (2015) Synthesis of 8-hydroxy-2-iminochromene derivatives as selective and potent inhibitors of human carbonyl reductase 1. *Org Biomol Chem* 13:7487–7499. <https://doi.org/10.1039/c5ob00847f>
- Boušová I, Skálová L, Souček P, Matoušková P (2015) The modulation of carbonyl reductase 1 by polyphenols. *Drug Metab Rev* 47:520–533. <https://doi.org/10.3109/03602532.2015.1089885>
- Yokoyama Y, Xin B, Shigeto T, Umemoto M, Kasai-Sakamoto A, Futagami M et al (2007) Clofibrilic acid, a peroxisome proliferator-activated receptor α ligand, inhibits growth of human ovarian cancer. *Mol Cancer Ther* 6:1379–1386. <https://doi.org/10.1158/1535-7163.MCT-06-0722>
- Umemoto M, Yokoyama Y, Sato S, Tsuchida S, Al-Mulla F, Saito Y (2001) Carbonyl reductase as a significant predictor of survival and lymph node metastasis in epithelial ovarian cancer. *Br J Cancer* 85:1032–1036. <https://doi.org/10.1054/bjoc.2001.2034>
- Miura R, Yokoyama Y, Shigeto T, Futagami M, Mizunuma H (2015) Inhibitory effect of carbonyl reductase 1 on ovarian cancer growth via tumor necrosis factor receptor signaling. *Int J Oncol* 47:2173–2180. <https://doi.org/10.3892/ijo.2015.3205>
- Kobayashi A, Yokoyama Y, Osawa Y, Miura R, Mizunuma H (2016) Gene therapy for ovarian cancer using carbonyl reductase 1 DNA with a polyamidoamine dendrimer in mouse models. *Cancer Gene Ther* 23:24–28. <https://doi.org/10.1038/cgt.2015.61>
- Nishimoto Y, Murakami A, Sato S, Kajimura T, Nakashima K, Yakabe K et al (2018) Decreased carbonyl reductase 1 expression promotes tumor growth via epithelial mesenchymal transition in uterine cervical squamous cell carcinomas. *Reprod Med Biol* 17:173–181. <https://doi.org/10.1002/rmb.2.12086>
- Kajimura T, Sato S, Murakami A, Hayashi-Okada M, Nakashima K, Sueoka K, Sugino N (2019) Overexpression of carbonyl reductase 1 inhibits malignant behaviors and epithelial mesenchymal transition by suppressing TGF- β signaling in uterine leiomyosarcoma cells. *Oncol Lett* 18:1503–1512. <https://doi.org/10.3892/ol.2019.10429>
- Takenaka K, Ogawa E, Oyanagi H, Wada H, Tanaka F (2005) Carbonyl reductase expression and its clinical significance in non-small-cell lung cancer. *Cancer Epidemiol Biomarkers Prev* 14:1972–1975. <https://doi.org/10.1158/1055-9965.EPI-05-0060>
- Ikawa M, Kominami K, Yoshimura Y, Tanaka K, Nishimune Y, Okabe M (1995) Green fluorescent protein as a marker in transgenic mice. *Dev Growth Differ* 37:455–459. <https://doi.org/10.1046/j.1440-169X.1995.t01-2-00012.x>
- Meng G (2018) TransGeneR: a one-stop tool for transgene integration and rearrangement discovery using sequencing data. *bioRxiv*. <https://doi.org/10.1101/462267>
- Tang WH, Shilov IV, Seymour SL (2008) Nonlinear fitting method for determining local false discovery rates from decoy database searches. *J Proteome Res* 7:3661–3667. <https://doi.org/10.1021/pr070492f>
- Sennels L, Bukowski-Wills JC, Rappsilber J (2009) Improved results in proteomics by use of local and peptide-class specific false discovery rates. *BMC Bioinformatics* 10:179. <https://doi.org/10.1186/1471-2105-10-179>
- Xia J, Psychogios N, Young N, Wishart DS (2009) MetaboAnalyst: a web server for metabolomic data analysis and interpretation. *Nucleic Acids Res* 37:W652–W660. <https://doi.org/10.1093/nar/gkp356>
- Chong J, Soufan O, Li C, Caraus I, Li S, Bourque G et al (2018) MetaboAnalyst 4.0: towards more transparent and integrative metabolomics analysis. *Nucleic Acids Res* 46:W486–W494. <https://doi.org/10.1093/nar/gky310>
- Hopp TP, Prickett KS, Price VL, Libby RT, March CJ, Pat Cerretti DP et al (1988) A short polypeptide marker sequence useful for recombinant protein identification and purification. *Nat Biotechnol* 6:1204–1210. <https://doi.org/10.1038/nbt1088-1204>
- Einhauser A, Jungbauer A (2001) The FLAG™ peptide, a versatile fusion tag for the purification of recombinant proteins. *J Biochem Biophys Methods* 49:455–465. [https://doi.org/10.1016/S0165-022X\(01\)00213-5](https://doi.org/10.1016/S0165-022X(01)00213-5)

24. Osawa Y, Yokoyama Y, Shigeto T, Futagami M, Mizunuma H (2015) Decreased expression of carbonyl reductase 1 promotes ovarian cancer growth and proliferation. *Int J Oncol* 46:1252–1258. <https://doi.org/10.3892/ijo.2014.2810>
25. Oikiri H, Asano Y, Matsusaki M, Akashi M, Shimoda H, Yokoyama Y (2019) Inhibitory effect of carbonyl reductase 1 against peritoneal progression of ovarian cancer: evaluation by ex vivo 3D-human peritoneal model. *Mol Biol Rep* 46:4685–4697. <https://doi.org/10.1007/s11033-019-04788-6>
26. Miyoshi I, Takahashi K, Kon Y, Okamura T, Mototani Y, Araki Y, Kasai N (2002) Mouse transgenic for murine oviduct-specific glycoprotein promoter-driven simian virus 40 large T-antigen: tumor formation and its hormonal regulation. *Mol Reprod Dev* 63:168–176. <https://doi.org/10.1002/mrd.10175>
27. Piska K, Koczurkiewicz P, Bucki A, Wójcik-Pszczola K, Kołaczkowski M, Pękala E (2017) Metabolic carbonyl reduction of anthracyclines - role in cardiotoxicity and cancer resistance. Reducing enzymes as putative targets for novel cardioprotective and chemosensitizing agents. *Investig New Drugs* 35:375–385. <https://doi.org/10.1007/s10637-017-0443-2>
28. Zhong L, Shen H, Huang C, Jing H, Cao D (2011) AKR1B10 induces cell resistance to daunorubicin and idarubicin by reducing C13 ketonic group. *Toxicol Appl Pharmacol* 255:40–47. <https://doi.org/10.1016/j.taap.2011.05.014>
29. Matsunaga T, Wada Y, Endo S, Soda M, El-Kabbani O, Hara A (2012) Aldo-keto reductase 1B10 and its role in proliferation capacity of drug-resistant cancers. *Front Pharmacol* 3:5. <https://doi.org/10.3389/fphar.2012.00005>
30. Stolarz AJ, Sarimollaoglu M, Marecki JC, Fletcher TW, Galanzha EI, Rhee SW et al (2019) Doxorubicin activates ryanodine receptors in rat lymphatic muscle cells to attenuate rhythmic contractions and lymph flow. *J Pharmacol Exp Ther* 371:278–289. <https://doi.org/10.1124/jpet.119.257592>
31. Arai Y, Endo S, Miyagi N, Abe N, Miura T, Nishinaka T et al (2015) Structure–activity relationship of flavonoids as potent inhibitors of carbonyl reductase 1 (CBR1). *Fitoterapia* 101:51–56. <https://doi.org/10.1016/j.fitote.2014.12.010>
32. Carlquist M, Frejd T, Gorwa-Grauslund MF (2008) Flavonoids as inhibitors of human carbonyl reductase 1. *Chem Biol Interact* 174:98–108. <https://doi.org/10.1016/j.cbi.2008.05.021>
33. Zemanova L, Hofman J, Novotna E, Musilek K, Lundova T, Havrankova J et al (2015) Flavones inhibit the activity of AKR1B10, a promising therapeutic target for cancer treatment. *J Nat Prod* 78:2666–2674. <https://doi.org/10.1021/acs.jnatprod.5b00616>
34. Huang W, Ding L, Huang Q, Hu H, Liu S, Yang X et al (2010) Carbonyl reductase 1 as a novel target of (-)-epigallocatechin gallate against hepatocellular carcinoma. *Hepatology* 52:703–714. <https://doi.org/10.1002/hep.23723>
35. Ito Y, Mitani T, Harada N, Isayama A, Tanimori S, Takenaka S et al (2013) Identification of carbonyl reductase 1 as a resveratrol-binding protein by affinity chromatography using 4'-amino-3,5-dihydroxy-trans-stilbene. *J Nutr Sci Vitaminol (Tokyo)* 59:358–364. <https://doi.org/10.3177/jnsv.59.358>
36. Hintzpeter J, Hornung J, Ebert B, Martin HJ, Maser E (2015) Curcumin is a tight-binding inhibitor of the most efficient human daunorubicin reductase - carbonyl reductase 1. *Chem Biol Interact* 234:162–168. <https://doi.org/10.1016/j.cbi.2014.12.019>
37. Hintzpeter J, Seliger JM, Hofman J, Martin HJ, Wsol V, Maser E (2016) Inhibition of human anthracycline reductases by emodin - A possible remedy for anthracycline resistance. *Toxicol Appl Pharmacol* 293:21–29. <https://doi.org/10.1016/j.taap.2016.01.003>
38. Gambliel HA, Burke BE, Cusack BJ, Walsh GM, Zhang YL, Mushlin PS, Olson RD (2002) Doxorubicin and C-13 deoxydoxorubicin effects on ryanodine receptor gene expression. *Biochem Biophys Res Commun* 291:433–438. <https://doi.org/10.1006/bbrc.2002.6380>
39. Hiller S, Abramson J, Mannella C, Wagner G, Zeth K (2010) The 3D structures of VDAC represent a native conformation. *Trends Biochem Sci* 35:514–521. <https://doi.org/10.1016/j.tibs.2010.03.005>
40. Freeland MM, Angulo J, Davis AL, Flook AM, Garcia BL, King NA et al (2012) Sex differences in improved efficacy of doxorubicin chemotherapy in *Cbr1*^{+/-} mice. *Anticancer Drugs* 23:584–589. <https://doi.org/10.1097/CAD.0b013e3283512726>
41. Arima-Yoshida F, Raveau M, Shimohata A, Amano K, Fukushima A, Watanabe M et al (2020) Impairment of spatial memory accuracy improved by *Cbr1* copy number resumption and GABAB receptor-dependent enhancement of synaptic inhibition in Down syndrome model mice. *Sci Rep* 10:14187. <https://doi.org/10.1038/s41598-020-71085-9>
42. Deutsch EW, Csordas A, Sun Z, Jarnuczak A, Perez-Riverol Y, Ternent T et al (2017) The ProteomeXchange Consortium in 2017: supporting the cultural change in proteomics public data deposition. *Nucleic Acids Res* 45:D1100–D1106. <https://doi.org/10.1093/nar/gkw936>
43. Okuda S, Watanabe Y, Moriya Y, Kawano S, Yamamoto T, Matsumoto M et al (2017) JPOSTrepo: an international standard data repository for proteomes. *Nucleic Acids Res* 45:D1107–D1111. <https://doi.org/10.1093/nar/gkw1080>

Publisher's Note Springer Nature remains neutral with regard to jurisdictional claims in published maps and institutional affiliations.

Springer Nature or its licensor holds exclusive rights to this article under a publishing agreement with the author(s) or other rightsholder(s); author self-archiving of the accepted manuscript version of this article is solely governed by the terms of such publishing agreement and applicable law.